

method, will be found in addition to UV detection. Then, the chemical composition of copolymers could be determined, directly, by dual detections. If the activity of adsorbent can be kept constant, moreover, the calibration curve of Figure 6 may be determined by independent experiments and, hence, the CCD of copolymers with broad distribution may be determined by the present method.

Acknowledgment. The authors wish to thank Professor Mitsuru Nagasawa of Nagoya University for his helpful discussion and Dr. Yoshio Kato of Toyo Soda Manufacturing Co., Ltd., for supplying the TSK-GEL columns. The present work was supported by a grant in aid for scientific research from the Ministry of Education, Science and Culture of Japan.

References and Notes

- (1) V. A. Agasandyan, L. G. Kudryavtseva, A. D. Litmanovich, and V. Ya. Shtern, *Vysokomol. Soedin., Ser. A*, **9**, 2634 (1967).
- (2) S. Teramachi and Y. Kato, *J. Macromol. Sci., Chem.*, **4**, 1785 (1970).
- (3) S. Teramachi and Y. Kato, *Macromolecules*, **4**, 54 (1971).
- (4) S. Teramachi and T. Fukao, *Polym. J.*, **6**, 532 (1974).
- (5) H. Inagaki, H. Matsuda, and F. Kamiyama, *Macromolecules*, **1**, 520 (1968).
- (6) J. Walchli, T. Miyamoto, and H. Inagaki, presented in ref 7.
- (7) H. Inagaki, *Adv. Polym. Sci.*, **24**, 189 (1977).
- (8) B. G. Belenkii and E. S. Gankina, *Dokl. Akad. Nauk SSSR*, **186**, 857 (1969); *J. Chromatogr.*, **53**, 3 (1970).
- (9) N. Tagata and T. Homma, *Nippon Kagaku Zasshi*, **1330** (1972).
- (10) J. L. White, D. G. Salladay, D. O. Quisenberry, and D. L. Maclean, *J. Appl. Polym. Sci.*, **16**, 2811 (1972).
- (11) S. Mori and T. Takeuchi, *Kobunshi Kagaku*, **29**, 383 (1972).
- (12) K. Kamide, S. Manabe, and E. Osafune, *Makromol. Chem.*, **168**, 173 (1973).
- (13) T. Kotaka and J. L. White, *Macromolecules*, **7**, 106 (1974).
- (14) S. Teramachi and H. Esaki, *Polym. J.*, **7**, 593 (1975).
- (15) S. Teramachi, A. Hasegawa, M. Akatsuka, A. Yamashita, and N. Takemoto, *Macromolecules*, **11**, 1206 (1978).
- (16) W. H. Stockmayer, *J. Chem. Phys.*, **13**, 199 (1945).
- (17) V. E. Meyer and G. G. Lowry, *J. Polym. Sci., Part A*, **3**, 2843 (1965).
- (18) F. R. Mayo and F. M. Lewis, *J. Am. Chem. Soc.*, **66**, 1594 (1944).

Surface Studies on Multicomponent Polymer Systems by X-ray Photoelectron Spectroscopy. Polystyrene/Poly(ethylene oxide) Triblock Copolymers

James J. O'Malley,^{1a} H. Ronald Thomas,* and Grace M. Lee^{1b}

Xerox Corporation, Webster Research Center, Rochester, New York 14644.

Received May 8, 1979

ABSTRACT: Angular-dependent X-ray photoelectron spectroscopy, XPS(θ), was used to determine the surface compositions and topographies of a series of PEO/PS/PEO triblock copolymer films cast from chloroform. The results indicate that the PS concentration at the air-polymer interface is substantially higher than the known bulk concentration of PS and that the copolymer surfaces are laterally inhomogeneous, i.e., there are isolated domains of PS and PEO residing at the surface. Furthermore, the molar composition of the surface corresponds to the surface area occupied by each component. A comparison of these results on triblock copolymers with those found earlier on the PS/PEO diblock copolymers indicates these two systems have remarkably similar surface compositions and topographies. This study has, for the first time, shown that data from XPS(θ) measurements can provide information bearing on the question of phase-separation behavior in multicomponent polymer systems. Our results on the triblock copolymers suggest that the components in the copolymers are partially miscible in the surface region and that this miscibility is a result of electronic interactions between the PEO and PS blocks in the copolymers.

In the first paper in this series,² we reported on our studies of the surface properties of polystyrene (PS)/poly(ethylene oxide) (PEO) diblock copolymers. Our results indicated that solvent-cast films had surface excesses of PS; i.e., the concentration of PS in the surface region at the air-polymer interface was higher than the concentration of PS in the bulk. Furthermore, the surfaces of the block copolymer films were shown to be laterally inhomogeneous in PS and PEO, and isolated domains of each of these components were present at the surface. These domains were found to extend more than 50 Å into the bulk. Models for the surface topography of the copolymers suggested that the surfaces were nonplanar and that the PS domains were elevated above the PEO domains.

The above experimental results, as well as those described in this paper, were obtained, using X-ray photoelectron spectroscopy (XPS) techniques. In the XPS experiment, one measures the binding energies of electrons ejected by the interaction of a molecule with a monoenergetic beam of soft X-rays.³ Information about the

surfaces of solids is derived from measurements of the absolute binding energies, relative kinetic energies, and peak intensities corresponding to the direct photoionization of the core levels (e.g., C_{1s} and O_{1s}). XPS is inherently sensitive to the surfaces (top few monolayers)³ of solids because of the very short (<100 Å) mean free paths for electrons and their strong dependence on kinetic energy.⁴⁻⁷ By coupling our knowledge of electron mean free paths in polymers with measurements of the angular dependence of the photoelectron spectra [XPS(θ)], it is possible to depth profile surface compositional variations and to model the morphology and topography of polymer surfaces.²

We now wish to report the results of further work on PS and PEO copolymers. In this paper, we have utilized XPS(θ) techniques to investigate the influence of chemical composition on the surface properties of solvent-cast PEO/PS/PEO triblock copolymer thin films. We will compare the current results on the triblock copolymers with those previously reported on the PS/PEO diblock copolymers of comparable composition in order to assess the influence of copolymer structure on the surface

Table I
Characterization Data for the
PEO/PS/PEO Triblock Copolymers

sample	% PS		segment $M_n \times 10^{-3}$
	wt	mol	PEO-PS-PEO
A	23.5	11.4	8.5–5.1–8.5
B	38.5	21.0	8.4–10.5–8.4
C	70.3	49.8	9.1–43.2–9.1

properties in this system. Finally, we will describe how our XPS(θ) results indicate differences in the phase-separation behavior of PS/PEO diblock and PEO/PS/PEO triblock copolymers.

Experimental Section

A. Synthesis of PEO/PS/PEO Triblock Copolymers. The triblock copolymers were synthesized by anionic polymerization techniques and purified by fractional precipitation. A detailed description of the synthesis and characterization of these copolymers can be found elsewhere.⁸ The bulk chemical compositions and number average weights for the three triblock copolymers used in this study are shown in Table I.

B. XPS Sample Preparation. Thin films ($\sim 5 \mu\text{m}$) of the block copolymers were prepared by dip coating them onto flat aluminum substrates from dilute, spectroscopic grade, chloroform (Burdick and Jackson) solutions. The films were dried in an Argon atmosphere at ambient temperature to reduce surface oxidation of the copolymers, and the Cl_{2p} core levels were monitored to ensure all residual chloroform was removed from the film before the XPS study was begun.

C. XPS Instrumentation. Spectra were recorded on an AEI ES200B spectrometer by using Mg $K\alpha_{1,2}$ exciting radiation. Typical operating conditions were: X-ray gun, 12 kV, 15 mA; pressure in the source chamber ca. 10^{-8} torr. Under the experimental conditions employed, the gold $4f_{7/2}$ level at 84 eV binding energy (BE) used for calibration had a full width at half-maximum (fwhm) of 1.2 ± 0.1 eV. No evidence was obtained for radiation damage to the sample from long-term exposure to the X-ray beam. Due to the rather long analysis times required for the angular-dependent studies, a liquid-nitrogen-cooled X-ray cap was used throughout the study to eliminate hydrocarbon contamination of the sample surface, and this device has been described in detail elsewhere.⁹

Calibration of the absolute energy scale was achieved by disconnecting the liquid-nitrogen cooling cap on the X-ray anode and allowing hydrocarbon contamination to collect on the sample surface. The value of 285.0 eV was used for the C_{1s} core level of the hydrocarbon, and the details of this method of calibration have been discussed elsewhere.⁶

Overlapping peaks were resolved into their individual components by use of a DuPont 310 curve resolver (an analog computer). The detailed deconvolutions were based on a knowledge of line widths determined from studies of homopolymers and model compounds.¹⁰ These studies have shown that for individual components of the core level spectra for C_{1s} and O_{1s} levels, the line shapes are approximately Gaussian.

Results and Discussion

Surface Composition. In the previous publication,² we analyzed the XPS spectra of the PS and PEO homopolymers, and they provide the basis for the current

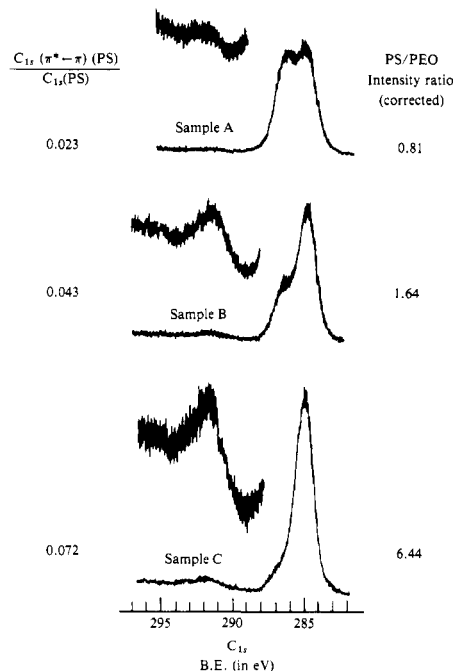


Figure 1. C_{1s} core level spectra for PEO/PS/PEO triblock copolymer samples A, B, and C.

interpretation of the triblock copolymers. Table II summarizes the relevant data on the two homopolymers. The major differences between PS and PEO include the 1.5 eV chemical shift in the C_{1s} core level spectra, the $\pi^* \leftarrow \pi$ shake-up peak uniquely attributable to PS, the O_{1s} core levels associated with PEO, and the relative peak intensity ratios for the C_{1s} core levels. The details of these results were discussed previously,² and they allow for an unambiguous analysis of the surface composition of the PEO/PS/PEO triblock copolymers.

Representative C_{1s} core level spectra for the three triblock copolymers are shown in Figure 1. The spectra show the characteristic chemical shift of about 1.5 eV for the C_{1s} levels associated with the PS and PEO components in the copolymers and the shake-up satellites at ~ 292 eV associated with the $\pi^* \leftarrow \pi$ transition in PS. The ratio of the shake-up peak intensity to the main C_{1s} peak intensity for the PS component in each of the copolymers is shown on the left-hand side of Figure 1. Surprisingly, this ratio was found to vary with copolymer composition. In a subsequent section on phase mixing, we will discuss the implications of this finding.

Through deconvolution of the C_{1s} spectra in Figure 1 and the application of the appropriate correction factors (Table II) for the signal intensities for each of the components, one can calculate the corrected intensity ratio of the PS and PEO peaks. These data are tabulated on the right-hand side of Figure 1. It is clear that the surface concentration of PS increases as the bulk concentration of PS increases in samples A–C. Figure 2 shows quantitatively the relationship between the surface and the bulk composition of the triblock copolymers. In the top 50 Å of

Table II
Experimental Binding Energies and Peak Area Ratios for the
Reference Homopolymers, Polystyrene and Poly(ethylene oxide)

	binding energy, ^a eV			peak area ratios
	C_{1s}	$\text{C}_{1s}(\pi^* \leftarrow \pi)$	O_{1s}	
polystyrene	285.0	291.6		$\text{C}_{1s}(\text{PS})/\text{C}_{1s}(\text{PEO}) = 1.60 \pm 0.1$
poly(ethylene oxide)	286.5		533.3	$\text{C}_{1s}(\text{PEO})/\text{O}_{1s}(\text{PEO}) = 0.73 \pm 0.05$
				$\text{C}_{1s}(\pi^* \leftarrow \pi)(\text{PS})/\text{C}_{1s}(\text{PS}) = 0.081 \pm 0.005$

^a Referenced to hydrocarbon at 285.0 eV.

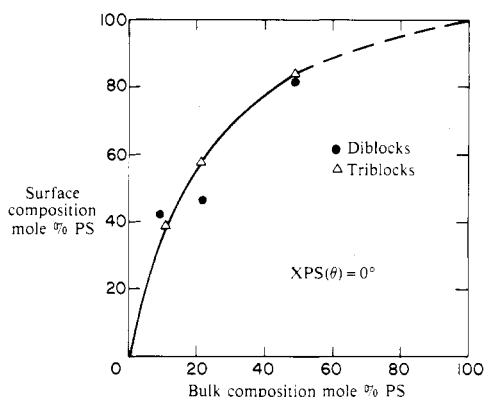


Figure 2. Surface vs. bulk compositions for PS/PEO diblock and PEO/PS/PEO triblock copolymer films cast from chloroform solutions.

these triblock copolymers, there is a significant surface excess of PS compared to the bulk. Figure 2 also contains comparable data for the PS/PEO diblock copolymers, taken from our earlier study,² and it is interesting to note the striking similarity in the surface behavior of the triblock and diblock copolymers.

Depth Profiling and Surface Topography. In the previous paper, we described the fundamentals and demonstrated the utility of angular-dependent XPS measurements, $XPS(\theta)$, in depth profiling the compositional variations of the diblock copolymers near the air-polymer interface.² Experimentally, the $XPS(\theta)$ measurements are made by rotating the sample relative to the fixed position electron analyzer and this, in effect, varies the sampling depth. The sampling depth is maximized when the electrons are collected normal ($\theta = 0^\circ$) to the sample surface and minimized as $\theta \rightarrow 90^\circ$. For C_{1s} electrons excited by $Mg K\alpha_{1,2}$ radiation, the inelastic mean free path is $\sim 15 \text{ \AA}$,⁷ and, therefore, about 95% of the signal arises from the top 50 \AA at $\theta = 0^\circ$ and from the top 10 \AA at $\theta = 80^\circ$. Thus, by taking spectra at angles of θ ranging from 0 – 80° , one can determine the average composition at each effective sampling depth and establish a composition–depth profile in the outermost 50 \AA of the sample. (Although the value of 15 \AA for the inelastic mean free path in ref 7 was determined on poly(*p*-xylylene), it is assumed this value will differ little for our system.)

In Figure 3 are shown the C_{1s} and O_{1s} core level spectra from an $XPS(\theta)$ study of sample B, which has a bulk composition of 21.0 mol % PS. The spectra were recorded at $\theta = 0, 45, \text{ and } 80^\circ$, and the C_{1s} core level spectra, as well as the corrected PS to PEO intensity ratios, show a progressive increase in PS concentration as θ is increased from 0 to 80° , thus indicating a compositional gradient in the outermost 50 \AA of the sample near the air–polymer interface. Figure 3 also contains the O_{1s} core level spectra for sample B as a function of θ and a tabulation of the C_{1s}/O_{1s} intensity ratios for the PEO component in the polymer. The measured values, ranging from 1.2–1.4, are significantly higher than the C_{1s}/O_{1s} intensity ratio of 0.73 found for PEO homopolymer. These data suggest there is some mixing of PS and PEO. A more detailed interpretation of these data will be proposed in the following section on phase mixing.

Table III contains the results of our $XPS(\theta)$ measurements on the surface-composition profile of the three triblock copolymers and, for comparative purposes, our earlier results² on the PS/PEO diblock copolymers. In general, the trends in both sets of copolymers are similar; i.e., there is a significant surface excess of PS at all copolymer compositions and angles θ , and there is a gradient

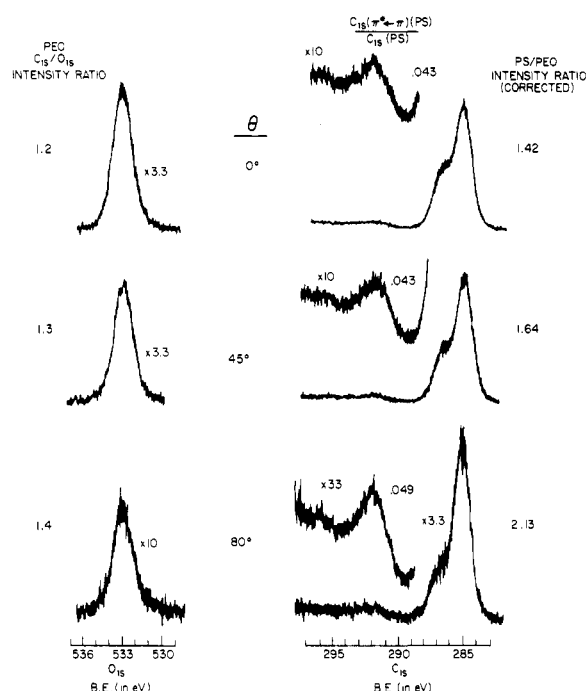


Figure 3. C_{1s} and O_{1s} core level spectra taken as a function of angle, θ , for PEO/PS/PEO triblock copolymer B cast from chloroform. The PS/PEO C_{1s} intensity ratios are corrected, using the ratios of the absolute signal intensities shown in Table II.

Table III
Surface Compositions of PS/PEO and PEO/PS/PEO Block Copolymer Films Determined by the $XPS(\theta)$ Technique

bulk comp (mol % PS)	copolymer type	surface comp by $XPS(\theta)$		
		$\theta = 0^\circ$	$\theta = 45^\circ$	$\theta = 80^\circ$
~10	diblock	42	54	62
	triblock	39	45	63
~20	diblock	46	52	56
	triblock	58	62	68
~50	diblock	82	85	86
	triblock	84	87	89

in surface composition in the top 50 \AA for all but the copolymers having ~ 50 mol % PS bulk compositions.

The similarity in the $XPS(\theta)$ data in Table III for the triblock and diblock copolymers indicates that the triblocks have surface topographies similar to those found earlier² for the diblocks. We can eliminate a continuous overlayer model,² in which PS would form a continuous surface overlayer on top of the PEO component, because we do not observe the predicted exponential dependence of the PS relative intensity as θ is varied from 0 to 80° . The evidence indicates that the PS and PEO components in the copolymers are both exposed at the surface and that they are organized into domains which are thick compared to the XPS sampling depth. The slight angular dependence we do observe as θ is varied again points to a nonplanar surface topography in which the PS domains are slightly elevated above the PEO domains, as described in the diblock copolymer paper.²

Phase Mixing. There have been numerous studies employing calorimetric,⁸ dynamic mechanical,¹¹ dielectric,¹² and morphological^{13,14} techniques to elucidate the solid-state behavior of styrene–ethylene oxide block copolymers. These measurements have focused on transition-temperature phenomena, and they have provided reference data on the bulk properties of the copolymers. The evidence accumulated to date indicates that PS and PEO are incompatible in the bulk. While this appears true, in

Table IV
XPS(θ) Data for PS, PEO, and the
PEO/PS/PEO Triblock Copolymers

sample	angle (θ), deg	C_{1s}/O_{1s} (PEO)	$\pi^* \leftarrow \pi /$ C_{1s} (PS)
PEO	0, 45, 80	0.73	
PS	0, 45, 80		0.075
PEO-PS-PEO	0	1.22	0.016
(11.4 mol % PS)	45	1.23	0.023
	80	1.22	0.032
PEO-PS-PEO	0	1.20	0.043
(21.0 mol % PS)	45	1.30	0.043
	80	1.40	0.049
PEO-PS-PEO	0	1.23	0.065
(49.8 mol % PS)	45	1.23	0.072
	80	1.23	0.075

general, one cannot rule out the possibility that PS and PEO have some limited degree of miscibility in the copolymers. It is also unknown, at this time, what influence an interface (e.g., the air-polymer interface) has on polymer-polymer compatibility and whether the degree of phase separation is the same or different in the bulk and in the surface. The present study, in part, addresses these issues by uniquely focusing on the surface properties rather than on the bulk properties of the copolymers. Our data suggest that, indeed, there is some compatibilization of PS in PEO.

In this section, we will discuss the interesting results, noted earlier, on the C_{1s}/O_{1s} intensity ratios for the PEO component and the $C_{1s}(\pi^* \leftarrow \pi)/C_{1s}$ intensity ratios for the PS component in the triblock copolymers. Table IV contains the measured intensity ratios for the two homopolymers and the three triblock copolymers. The triblocks deviate from the homopolymers in two ways: First, they have unusually high C_{1s}/O_{1s} ratios for the PEO component compared to the PEO homopolymer, and second, they have unusually low $C_{1s}(\pi^* \leftarrow \pi)/C_{1s}$ intensity ratios compared to the PS homopolymer. We will consider both of these significant deviations, in turn, and we will propose that these data are evidence of phase mixing in the solvent-cast PEO/PS/PEO triblock copolymer films.

Let us consider now the suggestion that the high C_{1s}/O_{1s} intensity ratio for the PEO component is due to partial phase mixing of PS and PEO. We can ask the question: "How much hydrocarbon would have to be intimately mixed with the PEO component to attenuate the oxygen signal of the PEO component and thereby effectively increase the C_{1s}/O_{1s} intensity ratio from 0.73 (PEO homopolymer) to the 1.2-1.4 range of values shown in Table IV for the copolymers?" In other words, what carbon to oxygen stoichiometries in a mixed phase of amorphous PEO and amorphous PS will result in measured C_{1s}/O_{1s} intensity ratios of 1.2-1.4? Using

$$C_{1s}/O_{1s}(\text{PEO in copolymer}) = x_c[C_{1s}/O_{1s}(\text{unmixed PEO})] + (1 - x_c)[C_{1s}/O_{1s}(\text{mixed PS-PEO})] \quad (1)$$

where the term on the left-hand side of eq 1 is the measured intensity ratio for the copolymer (values ranging from 1.2 to 1.4), x_c is the degree of crystallinity of the PEO

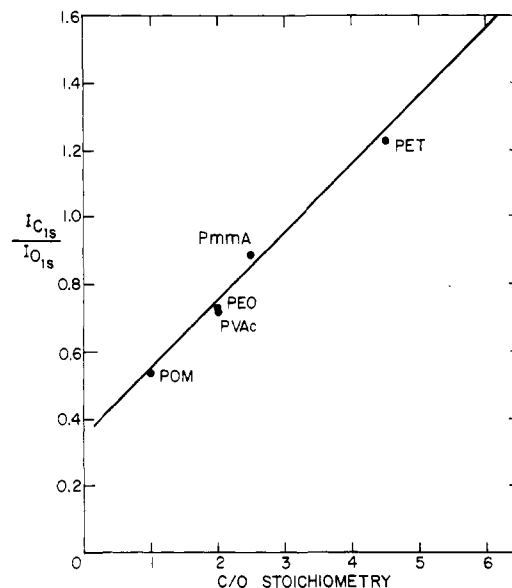


Figure 4. Calibration curve relating experimentally measured C_{1s}/O_{1s} intensity ratios to the known carbon-to-oxygen stoichiometries of a series of oxygen-containing homopolymers: POM, poly(oxyethylene); PVAc, poly(vinyl acetate); PEO, poly(ethylene oxide); PMMA, poly(methyl methacrylate); and PET, poly(ethylene terephthalate).

component measured by calorimetry⁸ and assumed to be the same for the surface region as for the bulk, and the term in the first bracket is the measured value of 0.73 for PEO homopolymer, we can calculate the term $C_{1s}/[O_{1s}(\text{mixed PS-PEO})]$, which is the intensity ratio for an intimate mixture of amorphous PEO and PS. To convert the calculated intensity ratios of the mixed phases in the copolymers into chemical compositions of the mixed phases, we need an experimental calibration curve relating these two quantities. This calibration curve is shown in Figure 4, in which we report C_{1s}/O_{1s} intensity ratios for a series of related homopolymers with known carbon to oxygen stoichiometries ranging from 1:1 in the case of poly(oxyethylene) to 4.5:1 in the case of poly(ethylene terephthalate). In using these polymers as model systems, we make the reasonable assumptions that the electron mean free paths differ insignificantly for these polymers at the same kinetic energy for photoemitted electrons and that the carbon and oxygen species are randomly arranged in the surface regions of these polymers.

The above procedure was used to calculate the composition of the mixed phase in each of the triblock copolymers. The results of the calculations are tabulated in Table V, and they show that the molar ratio of ethylene oxide to styrene in the mixed phase varies from 0.6:1 to 1.5:1 in going from sample A to C. Mixing of PS with amorphous PEO is most prevalent in sample A, which has the smallest concentration of PS and the shortest PS block length ($\bar{M}_n = 5.1K$). Almost 50% of the PS in the surface region of sample A films is mixed with PEO, whereas only 6% of the surface PS is mixed in sample C. It seems clear that PS and PEO are partially miscible in the surface regions of these triblock copolymers. Our finding that PS

Table V
Phase Mixing in PEO-PS-PEO Triblock Copolymers from Analysis of C_{1s}/O_{1s} (PEO) Intensity Ratios

surface comp (mol %)		deg of cryst (PEO)	mol % of PEO		E O/S comp (mixed phase)	mol % PS (mixed)	mol % PS (unmixed)
PS	PEO		cryst	amorp			
39.0	61.0	0.82	50	11.0	0.6/1	18.3	20.7
58.5	41.5	0.70	29	12.5	1.0/1	12.5	46.0
83.8	16.2	0.54	8.7	7.5	1.5/1	5.0	78.8

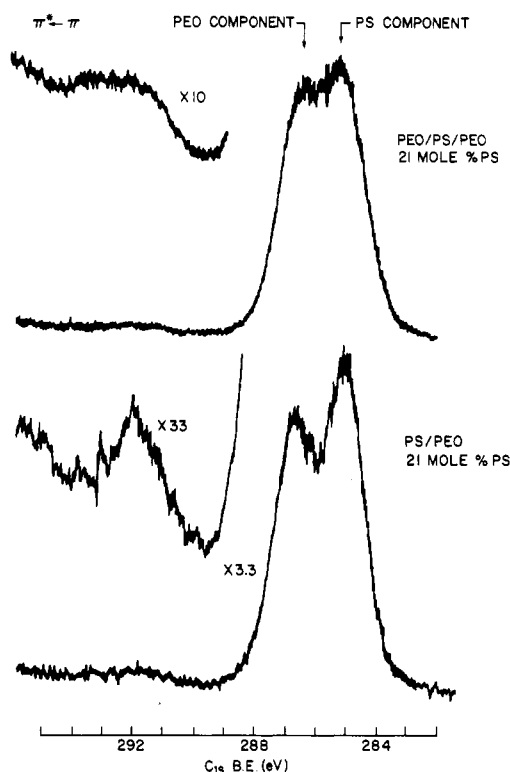


Figure 5. A comparison of the C_{1s} core level spectra and shake-up satellites found in PEO/PS/PEO triblock and PS/PEO diblock copolymers containing about 21 mol % PS.

is most miscible with PEO when the molecular weight and concentration of PS are low is qualitatively consistent with current concepts of phase-separation behavior in block copolymers¹⁵⁻¹⁷ and polyblends.¹⁸

Let us now turn our attention to other evidence bearing on the issue of phase mixing in PEO/PS/PEO copolymers. Inspection of the $C_{1s}(\pi^* \leftarrow \pi)/C_{1s}$ intensity ratios in Table IV reveals that these ratios decrease with decreasing PS concentration in the surface regions of the copolymers and that, for samples A and B, the ratios are significantly lower than the value of 0.75 for PS homopolymer. It is proposed that the low $C_{1s}(\pi^* \leftarrow \pi)/C_{1s}$ intensity ratios are a result of PS mixing with amorphous PEO in the surface and that the mixed PS and PEO components are electronically interacting. The effect of this interaction is to decrease the probability, relative to PS homopolymer, of a $\pi^* \leftarrow \pi$ transition occurring simultaneously with photoejection of a C_{1s} core level electron from a given aromatic ring in the copolymer.

Although the precise nature of the electronic interaction between PS and PEO is unknown at this time, we speculate that it involves the interaction of the electron-rich oxygen atoms in the PEO block with the aromatic rings in the PS portion of the copolymers. Based on the work of Dilks,¹⁹⁻²¹ which we will discuss in some detail below, we can anticipate that an electron donor/acceptor interaction between the ether oxygen in PEO and the phenyl rings in PS would result in (1) a shift in the PEO C_{1s} peak to lower binding energy because the influence of ether oxygen electrons on the adjacent carbon atoms in PEO is effectively being modulated by the interaction of these electrons with the phenyl ring in PS and (2) a change in the line shape for the $\pi^* \leftarrow \pi$ shake-up satellite peak. Both of these anticipated spectral changes are observed, as discussed below.

Figure 5 shows the C_{1s} core level spectra for a triblock copolymer and a diblock copolymer, both of which contain 21 mol % PS. Deconvolution and line-shape analysis of

the main C_{1s} envelope for each copolymer indicate that the full width at half-maximum of the individual component peaks does not vary with copolymer structure. However, there is an obvious "filling in" of the region between the two C_{1s} component peaks in the triblock copolymer spectrum. We attribute this to an additional PEO C_{1s} peak, shifted by about 0.3 eV to lower binding energy, that arises from an electronic interaction between PEO and PS.

Upon close inspection of the shake-up peaks for the diblock and triblock copolymers, shown in Figure 5, the shake-up peak associated with the triblock copolymer differs quite significantly from that found for the diblock. The shake-up peak shown in the diblock copolymer spectrum is virtually identical in line shape and intensity with that found in the polystyrene homopolymer.² The asymmetry to higher binding energy is due to the electronic transitions,¹⁹⁻²¹ $b^*_{1x} \leftarrow b_{1x}$ and $b^*_{1x} \leftarrow a_{2x}$, which are separated by only ~ 0.8 eV and have intensities of 3.3 and 4.8%, respectively, relative to the signal due to atoms in and attached to the phenyl ring. However, the shake-up peak associated with the triblock copolymer displays a distinct "doublet", rather than just an asymmetric structure, and a significantly decreased intensity relative to the primary PS C_{1s} core level peak. In seeking an explanation for this line shape and intensity change in the triblock copolymer shake-up peak, we turn to earlier studies by Dilks and Clark^{6,19-21} on the XPS spectra of para-substituted polystyrenes. These workers showed that para substitution of strong π -electron donor or acceptor groups on the phenyl groups in polystyrene resulted in a significant perturbation of the asymmetry of the shake-up peak. Additionally, the centroids of the satellite structure increased in energy separation with respect to the main C_{1s} peak as the para substituent was changed from a π -electron donor to a π -electron acceptor. Furthermore, Dilks and Clark^{6,19-21} found that the relative intensity of the $\pi^* \leftarrow \pi$ peak to the main C_{1s} photoionization peak depended on the nature of the para substituent; i.e., the $\pi^* \leftarrow \pi$ peak intensity decreased with increasing π -electron-donating power of the para substituent. Their results on poly(*p*-methoxystyrene) closely parallel our findings on the triblock copolymers. In the PEO/PS/PEO triblock copolymer system, the oxygen in the PEO component could act as an electron donor to the aromatic rings in PS, in a manner analogous to the poly(*p*-methoxystyrene) system. The manifestation of this electronic interaction would be the $\pi^* \leftarrow \pi$ energy shift (doublet structure) and the intensity decrease we observe for the triblock copolymer shake-up satellite peak in Figure 5.

These initial insights into electronic interactions of the components in the PEO/PS/PEO triblock copolymers and their role in polymer-polymer compatibility have instigated a rather intense study of similar systems involving PS derivatives and polyblends with polyethers. The results of these studies will be reported in the future.

Summary and Conclusions

XPS(θ) studies were used to determine the surface compositions and topographies of a series of PEO/PS/PEO triblock copolymer films cast from chloroform. The results indicate that the PS concentration at the air-polymer interface is substantially higher than the known bulk concentration of PS and that the copolymer surfaces are laterally inhomogeneous; i.e., there are isolated domains of PS and PEO residing at the surface. Furthermore, the molar composition of the surface corresponds to the surface area occupied by each component. A comparison of these results on triblock copolymers with those found earlier on the PS/PEO diblock copolymers indicates these two

systems have remarkably similar surface compositions and topographies.

This study has, for the first time, shown that data from XPS(θ) measurements can provide information bearing on the question of phase separation behavior in multicomponent polymer systems. Our results on the triblock copolymers clearly suggest that the components in the copolymers are partially miscible in the surface region and that this miscibility is a result of electronic interactions between the PEO and PS blocks in the copolymers. Additional studies to explore these interactions in related systems are warranted and are in progress.

Acknowledgment. We wish to extend our thanks to Drs. D. Shuttleworth, J. O'Reilly, and C. Beatty for helpful discussions, to Dr. C. B. Duke for encouragement and support, and to B. H. Fornalik for typing the manuscript.

References and Notes

- (1) (a) Exxon Chemical Co. P.O. Box 4255, Baytown, Tx. 77520; (b) Department of Biochemistry, Harvard University, Cambridge, Mass. 02138.
- (2) H. Ronald Thomas and J. J. O'Malley, *Macromolecules*, **12**, 323 (1979).
- (3) K. Siegbahn, C. Nordling, A. Fahlman, R. Nordberg, K. Hamrin, J. Hedman, G. Johansson, T. Berkmark, S. E. Karlsson, I. Lindgren, and B. Lindberg, "ESCA, Atomic, Molecular and Solid Structure Studied by Means of Electron Spectroscopy", Almquist and Wiksells, Uppsala, Sweden, 1967.
- (4) D. T. Clark, "Chemical Applications of ESCA in Electron Spectroscopy", W. Dekeyser, Ed., D. Reidel Publishing Co., Dordrecht, Holland, 1975, (NATO Summer School Lectures, Ghent, September 1972).
- (5) D. T. Clark, "Structure and Bonding in Polymers Revealed by ESCA in Electronic Structure of Polymers and Molecular Crystals", L. J. Andre, Ed., Plenum Press, New York, 1975 (NATO Summer School Lectures, Namur, September, 1974).
- (6) D. T. Clark, "Advances in Polymer Science", H.-J. Cantow et al., Eds., Springer-Verlag, Berlin, 1977.
- (7) D. T. Clark and H. R. Thomas, *J. Polym. Sci., Polym. Chem. Ed.*, **15**, 2843 (1977).
- (8) J. J. O'Malley, R. G. Crystal, and P. F. Erhardt in "Block Polymers", S. L. Aggarwal, Ed., Plenum Press, New York, 1970, pp 163–178.
- (9) D. T. Clark, H. R. Thomas, A. Dilks, and D. Shuttleworth, *J. Electron Spectrosc. Relat. Phenom.*, **10**, 455 (1977).
- (10) D. T. Clark and H. R. Thomas, *J. Polym. Sci., Polym. Chem. Ed.*, **14**, 1671 (1976).
- (11) P. F. Erhardt, J. J. O'Malley, and R. G. Crystal, ref 8, pp 195–211.
- (12) J. M. Pochan and R. G. Crystal in "Dielectric Properties of Polymers", F. E. Karasz, Ed., Plenum Press, New York, 1972, pp 313–327.
- (13) R. G. Crystal, P. F. Erhardt, and J. J. O'Malley, ref 8, pp 179–193.
- (14) R. G. Crystal in "The Colloidal and Morphological Properties of Block and Graft Copolymers", G. Molav, Ed., Plenum Press, New York, 1971, pp 279–293.
- (15) D. J. Meier, *J. Polym. Sci., Part C*, **26**, 81 (1969).
- (16) D. J. Meier, *Polym. Prepr., Am. Chem. Soc., Div. Polym. Chem.*, **11**, 400 (1970).
- (17) S. Krause, *Macromolecules*, **3**, 84 (1970).
- (18) I. Sanchez in "Polymer Blends", Vol. 1, D. Paul, Ed., Academic Press, New York, 1978, pp 115–139.
- (19) A. Dilks, Ph.D. Thesis, University of Durham, U.K., 1977.
- (20) D. T. Clark and A. Dilks, *J. Polym. Sci., Polym. Chem. Ed.*, **14**, 533 (1976).
- (21) D. T. Clark and A. Dilks, *J. Polym. Sci., Polym. Chem. Ed.*, **15**, 15 (1977).

Studies on the Conformation of Heparin by ^1H and ^{13}C NMR Spectroscopy

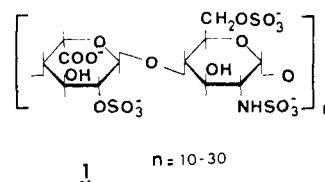
G. Gatti,^{*1a} B. Casu,^{1b} G. K. Hamer,^{1c} and A. S. Perlin^{1c}

Istituto Chimica Macromolecole CNR, 20133, Milano, Italy, Istituto di Chimica e Biochimica "G. Ronzoni", 20133, Milano, Italy, and Department of Chemistry, McGill University, Montreal, Canada H3A 2A7. Received April 16, 1979

ABSTRACT: A convolution-difference 270-MHz ^1H NMR spectrum of heparin has afforded a complete set of interproton coupling data for the major constituent residues of heparin, i.e., α -L-idopyranosyluronic acid 2-sulfate and 2-deoxy-2-sulfamino- α -D-glucopyranose 6-sulfate. According to these data, the conformation of the iduronic acid residue is $^1\text{C}_4(\text{L})$ or a slightly distorted form thereof, whereas that of the aminodeoxyhexose residue is $^4\text{C}_1(\text{D})$; the exocyclic $\text{CH}_2\text{OSO}_3^-$ group of the latter residue favors the gauche, gauche rotamer. The 5-proton of each residue exhibits selective line broadening and a large chemical shift displacement in the pK_a region of the uronide carboxyl group, which indicates that these particular protons are in close proximity within the molecule. This observation helps to define a solution conformation for the polyelectrolyte chain. Other information on stereochemical aspects, and on pH and temperature effects, is provided by ^{13}C NMR spectra. The latter are utilized also to highlight differences between beef lung (B type) and hog mucosal (A type) heparins, associated with the presence of minor constituent sugar residues, particularly through the acquisition of a difference ^{13}C spectra. It is also shown that signal dispersion in ^{13}C spectra of heparin is satisfactory at relatively low field (22.6 MHz) as well as at 67.9 MHz, provided that conditions of pH and ionic strength are optimized.

Heparin is a carbohydrate polymer that is widely distributed in animal tissues and is best known for its use in therapy as a blood anticoagulant. It is classed^{2,3} as a mucopolysaccharide, or glycosaminoglycan, although it also may be aptly described as a glycosaminoglycuronan since it is formally a copolymer of a hexosamine and a uronic acid.

Most of the heparin molecule is accounted for⁴⁻⁶ by repeating disaccharide unit 1 that consists of a residue of α -L-idopyranosyluronic acid 2-sulfate and of 2-deoxy-2-



sulfamino- α -D-glucopyranose 6-sulfate, each of which is glycosidically linked through position 4. This repeating sequence represents⁷⁻⁹ at least 85% of heparins from beef